

Anisotropy in magnetic dynamics of $\text{YBa}_2\text{Cu}_3\text{O}_7$

J. M. Rendell and J. P. Carbotte

Department of Physics and Astronomy, McMaster University, Hamilton, Ontario, Canada L8S 4M1

(Received 13 November 1995)

$\text{YBa}_2\text{Cu}_3\text{O}_7$ has orthorhombic symmetry because of the chains. The superconducting energy gap, which would have pure $d_{x^2-y^2}$ symmetry in the tetragonal case, is expected to also contain a small $s_{x^2+y^2}$ component in the orthorhombic case. This admixture shifts the gap nodes off the main diagonals and leads to a momentum space anisotropy in the spin dynamics. Recent neutron scattering results on the 41 meV peak in twinned crystals of $\text{YBa}_2\text{Cu}_3\text{O}_7$ are consistent with our results. Extension to untwinned crystals might be used to determine the amount of s -wave admixture although the interpretation is complicated by band anisotropy.

The spin dynamics of the high- T_c oxide superconductors and, in particular, of Y-Ba-Cu-O, is of great interest and has been extensively studied.¹⁻⁵ Very recently, the nature of the 41 meV neutron scattering peak in $\text{YBa}_2\text{Cu}_3\text{O}_7$ has been clarified.⁶ This large peak, which grows in the superconducting state as the temperature is reduced, has been identified with spin scattering (spin fluctuations) (Refs. 6,8,9) and is consistent with the opening up of a superconducting gap which has d -wave, $d_{x^2-y^2} \equiv [\cos(k_x) - \cos(k_y)]$ symmetry. Here k_x and k_y are momenta in the two-dimensional Brillouin zone of the CuO_2 plane. A successful model, which is often used to describe the spin susceptibility in the oxides, involves the bare noninteracting susceptibility (χ_0) calculated in the random phase approximation (RPA) for a tight binding band with a realistic Fermi surface which is further enhanced by correlations.¹⁰⁻¹⁷ Depending on the details of the model envisaged, the denominator in the RPA susceptibility, which gives the Stoner enhancement, can involve a constant Coulomb repulsion U or a structural function $U_{\mathbf{q}}$ of the form $U[\cos(q_x) + \cos(q_y)]$. In the first case, the constant U is usually thought to be large, leading to a large Stoner enhancement, and the oxides are envisaged as falling near their antiferromagnetic transition: the nearly antiferromagnetic Fermi liquid model (NAFFLM). In the second case, the oxides are not thought to be particularly near their magnetic transition. Instead, they have a modest Stoner enhancement and the factor $U_{\mathbf{q}}$ models incipient localization effects.

Very recently, Dai *et al.*⁷ have studied the momentum space behavior of the 41 meV neutron scattering peak in $\text{YBa}_2\text{Cu}_3\text{O}_7$ and have found that it is anisotropic. The width of the measured peak along the diagonal is different from that along the face of the Brillouin zone. The data are taken from twinned samples and correspond to some average over k_x and k_y direction which restores tetragonal symmetry although $\text{YBa}_2\text{Cu}_3\text{O}_7$ contains a CuO plane of chains besides the usual CuO_2 planes and this must have some effect on its superconducting properties. The simplest model that one can envisage, and which might be used as a first approximation to describe the physics of such a composite system of planes plus chains with several Fermi surface sheets, is a single band model but with a different hopping parameter for the x and the y (along the chain) directions. This simplified model,

while crude, captures the orthorhombicity of the system and leads to solutions¹⁸⁻²⁰ of the BCS gap equation for the NAF-FLM which contains an admixture of extended s -wave symmetry, $s_{x^2+y^2} = [\cos(k_x) + \cos(k_y)]$, as well as $d_{x^2-y^2}$ symmetry. The amount of the admixture increases with increasing orthorhombic distortion.¹⁸⁻²⁰ In the NAF-FLM, the pairing is assumed to proceed through the magnetic susceptibility which has been modeled by Millis, Monien, and Pines²¹ (MMP) on the basis of NMR data. Retaining the MMP model susceptibility unchanged in the BCS gap equations¹⁸⁻²⁰ but including the lattice orthorhombicity in the band structure immediately implies and fixes the amount of extended s -wave admixture in the gap. The details of the BCS solutions in the NAF-FLM are found in Refs. 18-21 and do not concern us directly here. It is sufficient to know that a 25% admixture of $s_{x^2+y^2}$ component in an otherwise $d_{x^2-y^2}$ superconductor is enough to explain the magnitude of the c -axis Josephson tunneling current observed by Sun *et al.*²² between $\text{YBa}_2\text{Cu}_3\text{O}_7$ and Pb as well as that observed in plane penetration depth anisotropy.¹⁷ This sets the scale of the possible $s_{x^2+y^2}$ component. Here we are interested in studying how this admixture of an $s_{x^2+y^2}$ component, which shifts the gap nodes off the main diagonals of the two-dimensional copper oxide Brillouin zone, leads to anisotropy in the spin susceptibility and how this asymmetry can be differentiated from band structure effects.

We start with a single band model for the electronic structure of $\text{YBa}_2\text{Cu}_3\text{O}_7$ but include an orthorhombic distortion so as to crudely model the chains through the introduction of an anisotropy parameter δ in the in-plane first nearest neighbor hopping parameter. This makes the k_x and k_y directions distinct in the two-dimensional copper oxide Brillouin zone. In this model, the electron energy $\epsilon_{\mathbf{k}}$, in tight binding, is taken to be of the form

$$\epsilon_{\mathbf{k}} = -2t[\cos(k_x) + (1 + \delta)\cos(k_y)] + 4tB \cos(k_x)\cos(k_y) - \mu, \quad (1)$$

where t is the size of the in-plane nearest neighbor hopping and B is the second nearest neighbor in units of t . The

chemical potential in Eq. (1) is μ and is related to the (single spin) filling $\langle n \rangle$ (half-filling: $\langle n \rangle = 0.5$) through the equation

$$\langle n \rangle = \frac{1}{2\Omega} \sum_{\mathbf{k}} \left[1 - \frac{\epsilon_{\mathbf{k}}}{E_{\mathbf{k}}} \tanh \left(\frac{E_{\mathbf{k}}}{2k_B T} \right) \right]. \quad (2)$$

Equation (2) for the filling $\langle n \rangle$ is already written for the superconducting state with $E_{\mathbf{k}} = \sqrt{\epsilon_{\mathbf{k}}^2 + \Delta_{\mathbf{k}}^2}$ where $\Delta_{\mathbf{k}}$ is the superconducting energy gap. The sum in (2) is over the first Brillouin zone, Ω is the normalizing volume, and T is the temperature. For $\delta=0$ in Eq. (1), the system is tetragonal and the solution of the BCS gap equation with the model susceptibility of Millis, Monien, and Pines²¹ (MMP) leads directly to a gap which exhibits pure $d_{x^2-y^2}$ symmetry.¹⁸⁻²⁰ Such solutions contain many of the higher harmonics of the $d_{x^2-y^2}$ irreducible representation of the crystal lattice point group but, for many purposes, the solutions can be represented by the lowest harmonic, namely

$$d_{x^2-y^2} = \cos(k_x) - \cos(k_y). \quad (3a)$$

This will be sufficient here. Once $\delta \neq 0$ in Eq. (1), however, the solutions of the BCS gap equation with MMP susceptibility no longer exhibit pure $d_{x^2-y^2}$ symmetry but contain an admixture of $s_{x^2+y^2}$, which can also be represented approximately by its lowest harmonic, namely¹⁸⁻²⁰ by

$$s_{x^2+y^2} = \cos(k_x) + \cos(k_y). \quad (3b)$$

The reader is referred to our previous work for further details.¹⁷⁻¹⁹ Once the gap $\Delta_{\mathbf{k}}$ is known, the spin susceptibility follows.

The bare single spin susceptibility in the superconducting state for momentum transfer \mathbf{q} and energy ω is given by

$$\chi_0(\mathbf{q}; \omega) = \frac{1}{4\Omega} \sum_{\mathbf{k}} \left\{ a_+(\mathbf{k}, \mathbf{q}) [f(E_{\mathbf{k}+\mathbf{q}}) - f(E_{\mathbf{k}})] \left(\frac{1}{\omega - (E_{\mathbf{k}+\mathbf{q}} - E_{\mathbf{k}}) + i\Gamma} - \frac{1}{\omega + (E_{\mathbf{k}+\mathbf{q}} - E_{\mathbf{k}}) + i\Gamma} \right) \right. \\ \left. + a_-(\mathbf{k}, \mathbf{q}) [1 - f(E_{\mathbf{k}+\mathbf{q}}) - f(E_{\mathbf{k}})] \left(\frac{1}{\omega + (E_{\mathbf{k}+\mathbf{q}} + E_{\mathbf{k}}) + i\Gamma} - \frac{1}{\omega - (E_{\mathbf{k}+\mathbf{q}} + E_{\mathbf{k}}) + i\Gamma} \right) \right\}, \quad (4)$$

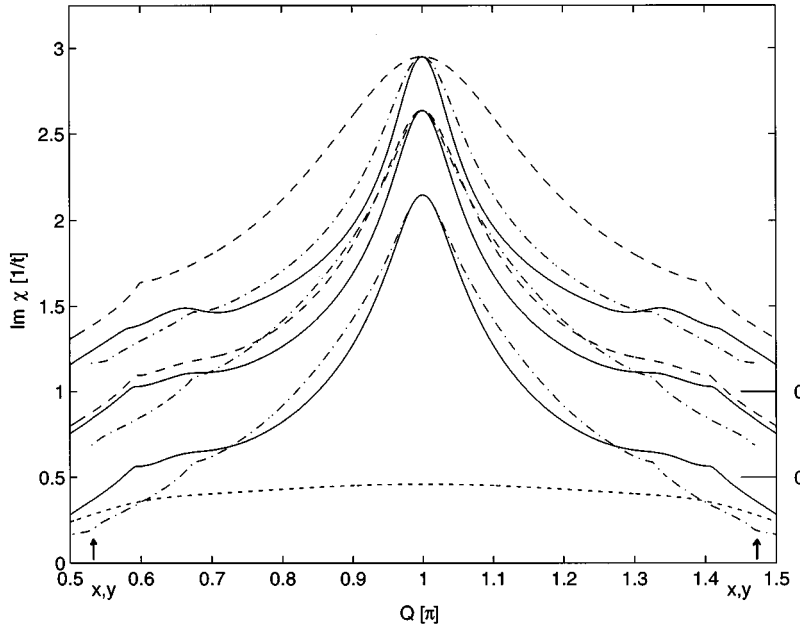


FIG. 1. The imaginary part of the spin susceptibility $\chi(\mathbf{q}; \omega)$ at $\omega = 0.347t$ for the two lower sets of curves and $\omega = 0.348t$ for the uppermost set shown as a function of momentum, q_x along (Q, π) (solid), the diagonal line, (Q, Q) (dash-dotted) and q_y along (π, Q) (dashed) in the interval 0.5π to 1.5π . The underlying lattice is tetragonal with next neighbor hopping $B = 0.45$, filling $\langle n \rangle = 0.4$ and $U = 1.0t$ with $\Gamma = 0.01t$. The first Brillouin zone has $(1000)^2$ points, the maximum value of $2\Delta_0$ (Brillouin zone) $= 0.4t$, and $T_c = 0.1t$. The lowest set is for a pure $d_{x^2-y^2}$ gap; the x and y directions are identical and the normal state result is also shown (dotted curve). The diagonal peak is wider than the x axis peak. The middle pair of curves are for $0.2s_{x^2+y^2} + 0.8d_{x^2-y^2}$. The asymmetry is already clear with a broader line in the diagonal and the y direction than in the x direction. This broadening is quite large in the upper pair of curves which apply for $0.5d_{x^2-y^2} + 0.5s_{x^2+y^2}$. Each set of curves is displaced upwards by half a unit; relative zeros are shown on the right-hand axis.

where $f(E)$ is the Fermi Dirac distribution function at finite temperature and Γ is a damping factor needed in the numerical work and taken to be $\Gamma=0.01t$ in the numerical data presented in this paper.

The full spin susceptibility in random phase approximation, enhanced by the Coulomb interactions, which we denote by $\chi(\mathbf{q};\omega)$, is given by

$$\chi(\mathbf{q};\omega) = \frac{\chi_0(\mathbf{q};\omega)}{1 + U_q \chi_0(\mathbf{q};\omega)}, \quad (5)$$

where U_q can be taken as a constant (the negative of the Hubbard U), as was done in many previous works,¹⁴⁻¹⁷ or as a function of the form

$$U_q = U[\cos(q_x) + \cos(q_y)]. \quad (6)$$

This form has been used extensively by Levin and collaborators.⁸⁻¹³ Here we will follow their lead and present results only for U_q of the form given by Eq. (6) although we have also obtained similar results with a constant value of U . The advantage of model (6) is that it preferentially enhances the peak at (π,π) when the spin susceptibility of Eq. (5) is calculated. We have found, however, that such peaks can also be obtained with constant U , particularly for the orthorhombic lattice.

Our results for the imaginary part of the spin susceptibility with $U=1.0t$, $B=0.45$, and $\delta=0$ (tetragonal case for the

electron dispersion) with a maximum gap on the Fermi surface value of $2\Delta_0=35.8$ meV on a mesh with $(1000)^2$ points are presented in Fig. 1. We show the momentum space dependence of $\text{Im}\chi(\mathbf{q},\omega)$ for ω fixed at the frequency which gives the maximum imaginary part of the susceptibility at (π,π) in the superconducting state at zero temperature and with $U=1.0t$ (see Fig. 4). The lines are marked as follows: normal state, along q_x or q_y axis at $T=T_c$ is dotted; the remaining lines are for the superconducting state at $T=0$. The solid lines are along (Q,π) , the dash-dotted lines are along (Q,Q) , and the dashed lines are along (π,Q) . The approximate positions of the pseudonesting peaks on the q_x , q_y axis (arrows) are also shown. The lowest set of superconducting lines, with the normal state shown for comparison, are for the pure d -wave energy gap at frequency $\omega=0.347t$. Note, the width of the peak in the diagonal direction is wider than that along (Q,π) or (π,Q) (tetragonal symmetry). This corresponds to the recent results of Dai *et al.*⁷ who used neutron scattering to study a large twinned crystal of $\text{YBa}_2\text{Cu}_3\text{O}_7$. They quote the corrected ratios of full width at half maximum (FWHM) of the diagonal peak to the on-axis peak as $0.51/0.38 \sim 1.4$. Our ratio is 1.2 for the $d_{x^2-y^2}$ case which is smaller than observed but of the correct order of magnitude. In making such a comparison, it should be pointed out that both measured peaks are much broader than found in our present calculation,^{8,9} and considerable caution should be exercised in such a comparison.

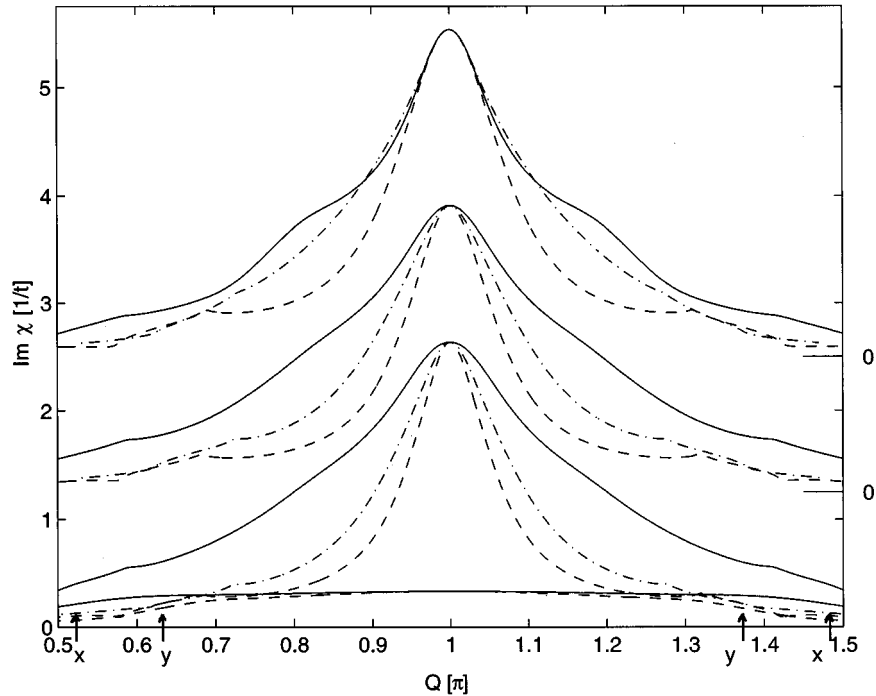


FIG. 2. The imaginary part of the spin susceptibility $\chi(\mathbf{q};\omega)$ as a function of momentum q_x along (Q,π) (solid), diagonal line, (Q,Q) (dash-dotted) and q_y along (π,Q) (dashed) in the interval 0.5π to 1.5π . The two almost flat curves at the bottom are the profiles at $T=T_c$. The frequencies are $\omega=0.347t$ for the lower curves, $\omega=0.357t$ for the middle curves, and $\omega=0.382t$ for the upper curves. The underlying lattice is orthorhombic in a one band model for the electronic system with finite value of the distortion parameter $\delta=0.25$ in Eq. (1) for the electric energies with $B=0.45$, filling $\langle n \rangle=0.4$, $U=1.0t$, $\Gamma=0.01t$, $T_c=0.1t$, maximum $2\Delta_0$ (Brillouin zone) $=0.4t$, and the first Brillouin zone has $(1000)^2$ points. The lowest set of curves is for pure $d_{x^2-y^2}$ gap symmetry. The x direction is much broader than the y direction. The middle curves are for $0.2s_{x^2+y^2} + 0.8d_{x^2-y^2}$. Relative to the pure d -wave case, the x axis line has sharpened while the y axis has broadened through the admixture of some $s_{x^2+y^2}$ component to the gap. The top set of curves is for $0.5s_{x^2+y^2} + 0.5d_{x^2-y^2}$. Each set of curves is displaced upwards by 1.25 units; relative zeros are shown on the right-hand side.

The next set of curves, displaced upwards by one unit for clarity, shows the profiles of the (π, π) peak for an admixture of 20% $s_{x^2+y^2}$ and 80% $d_{x^2-y^2}$ at frequency $\omega=0.347t$. Tetragonal symmetry has been broken—the profiles along (Q, π) (solid) and (π, Q) (dashed) are quite different. The diagonal line (dash-dotted) is near the y axis results.

The top set of curves, again displaced upwards, shows the profiles for a 50% $s_{x^2+y^2}+50\%$ $d_{x^2-y^2}$ energy gap at frequency $\omega=0.348t$. The q_y -axis peak (dashed line) is substantially wider than that of the q_x axis (solid line), showing considerable anisotropy in momentum space. In an experiment on twinned crystals, the zone face data will be an average of our x - and y -axis results if we assume equal weights of both twins. Since anisotropy between diagonal and face measurements is already expected for a pure d -wave case, it is not possible to fix the amount of extended s -wave admixture from such measurements. The situation is more favorable in untwinned crystals for which we predict a difference in FWHM between x - and y -axis measurements which increases with percent admixture of extended s wave. Such an effect is nonexistent in pure d wave. For an admixture between 20% and 50%, the predicted differences between x and y axis are of the same order and bigger than detected in the twinned crystal measurements of Dai *et al.*⁷

In Fig. 2, we show the profiles of the (π, π) peak of the imaginary part of the spin susceptibility for the specific case $\delta=0.25$ and for the neutron energy chosen to correspond to the maximum in the curves of Fig. 4 and similar curves for the other energy gaps. The filling is kept at $\langle n \rangle=0.4$, the maximum gap on the Fermi surface $2\Delta_0=38.9$ meV, and U in formula (6) is taken to have a value of $1.0t$. The calculations are done on a mesh of $(1000)^2$ points. The solid curves are lines in the Brillouin zone along (Q, π) , the dash-dotted curves along (Q, Q) , and the dashed curves along (π, Q) for the superconducting state at zero temperature with various frequencies and energy gaps. The arrows indicate the approximate positions of the nesting peaks, now different, on the x and y axis.

The two flat lines at the bottom are for the normal state of $T=T_c$. Already, the two curves are different because of the orthorhombic lattice. This is a sure sign of what we have called lattice anisotropy and would not exist in a tetragonal lattice. The lowest set of curves is for a pure d -wave energy gap, at frequency $\omega=0.347t$. The x axis peak (solid line) is now much wider than the y axis peak (dashed line). This is opposite to the tetragonal case discussed with Fig. 1. The second set of curves shows the peak widths for 20% $s_{x^2+y^2}$ and 80% $d_{x^2-y^2}$ at a frequency $\omega=0.357t$. The third set depicts equal amounts of $s_{x^2+y^2}$ and $d_{x^2-y^2}$ at a frequency of $\omega=0.382t$. We suggest polarized neutron scattering on an untwinned crystal of YBCO would produce similar curves to those displayed in Fig. 2. The band structure anisotropy has a distinct effect on the FWHM of the (π, π) peak—even with a symmetric, pure d -wave energy gap. A detailed analysis of the above results is now offered.

In Fig. 3, we look at the temperature dependence of the ratios of the FWHM in the q_x direction to that of the q_y direction in the first three rows of frames and the change in height at (π, π) with respect to the height at T_c in the bottom two frames (d) and (h). The left column describes a system with a tetragonal lattice and maximum gap on the Fermi

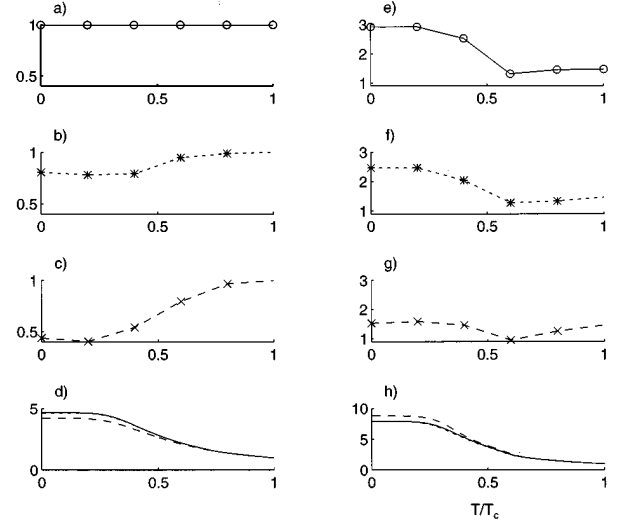


FIG. 3. Frames (a)–(c), (e)–(g) show the ratio of q_x FWHM to q_y FWHM vs reduced temperature for a tetragonal ($\delta=0$) lattice (left column) and orthorhombic ($\delta=0.25$) lattice (right column). The energy gaps are depicted by d -wave (solid lines), $0.25s_{x^2+y^2} + 0.8d_{x^2-y^2}$ (dotted line), and $0.5s_{x^2+y^2} + 0.5d_{x^2-y^2}$ (dashed lines). Frames (d) and (h) show the change in height with respect to the height at T_c vs reduced temperature for the tetragonal and orthorhombic lattice, respectively. Other parameters are $(1000)^2$ points in the first Brillouin zone, maximum $2\Delta_0$ (Brillouin zone)= $0.4t$, $T_c=0.1t$, $\Gamma=0.01t$, $B=0.45$, $\langle n \rangle=0.4$, and $U=1.0t$. For the tetragonal lattice ($\delta=0$), the frequencies are $\omega=0.347t$ (d -wave and $0.2s_{x^2+y^2} + 0.8d_{x^2-y^2}$ energy gaps) and $\omega=0.348t$ ($0.5s_{x^2+y^2} + 0.5d_{x^2-y^2}$ energy gap). For the orthorhombic lattice ($\delta=0.25$), the frequencies are $\omega=0.347t$ (d -wave energy gap), $\omega=0.357t$ ($0.2s_{x^2+y^2} + 0.8d_{x^2-y^2}$ energy gap), and $\omega=0.382t$ ($0.5s_{x^2+y^2} + 0.5d_{x^2-y^2}$ energy gap).

surface $2\Delta_0=35.8$ meV, and the right, a system with an orthorhombic lattice ($\delta=0.25$) and maximum gap on the Fermi surface $2\Delta_0=38.9$ meV. Common parameters are next nearest neighbor hopping $B=0.45$, filling $\langle n \rangle=0.4$, potential $U=1.0t$, smearing $\Gamma=0.01t$, $T_c=0.1t$, and mesh $(1000)^2$ points. In frame (a), we see the ratio of peak widths on a tetragonal lattice with a pure d -wave gap (open circles and solid line) and frequency $\omega=0.397t$. The ratio is constant at all temperatures—there is no anisotropy in the system. Frames (b) and (c) show the ratios for anisotropic d -wave gaps, $0.2s_{x^2+y^2} + 0.8d_{x^2-y^2}$ (*, dotted line; $\omega=0.347t$) and $0.5s_{x^2+y^2} + 0.5d_{x^2-y^2}$ (×, dashed line; $\omega=0.348t$), respectively. In each case, the widths of the peaks split into different values as the system moves into a superconducting state. The difference in the widths of the peaks is much greater for $0.5s_{x^2+y^2} + 0.5d_{x^2-y^2}$ energy gap at low temperatures (55%) than for the $0.2s_{x^2+y^2} + 0.8d_{x^2-y^2}$ energy gap (20%). Frame (e) shows the peak width ratios for an orthorhombic lattice and a pure d -wave energy gap (○, solid line) at frequency $\omega=0.347t$. The q_x profile is wider than the q_y at T_c ; this difference increases considerably at low temperatures. Frames (f) and (g) show anisotropic d -wave gaps on an orthorhombic lattice, $0.2s_{x^2+y^2} + 0.8d_{x^2-y^2}$ (*, dotted line; $\omega=0.357t$) and $0.5s_{x^2+y^2} + 0.5d_{x^2-y^2}$ (×, dashed line; $\omega=0.382t$), respectively. At low temperatures, as the anisotropy of the gap is increased, the difference in the peak profiles FWHM reduces. Frames (d) and (h) show the change in

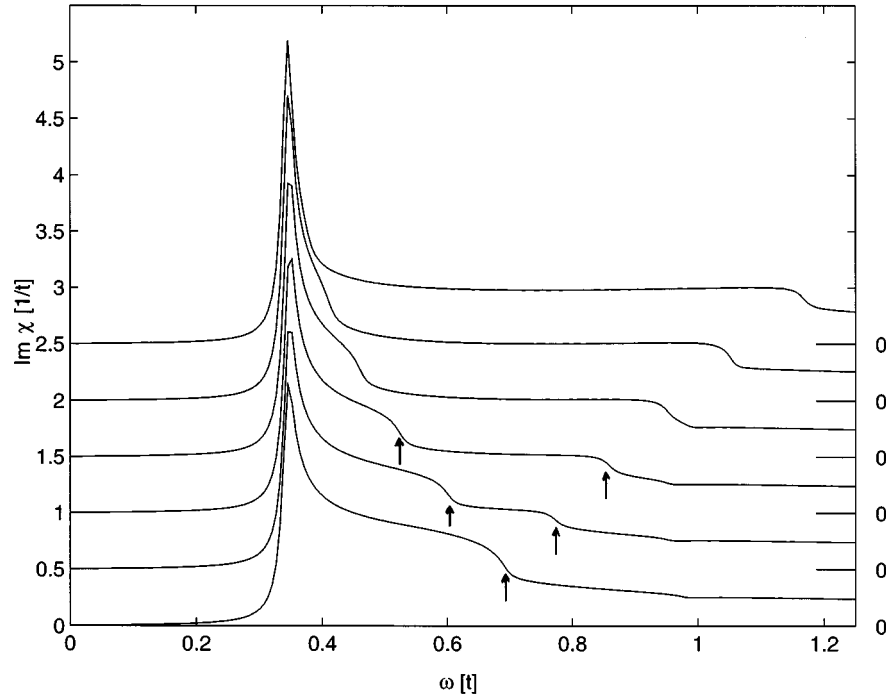


FIG. 4. Imaginary part of the single spin susceptibility at $\mathbf{q}=(\pi,\pi)$ as a function of energy (ω) normalized by the hopping energy (t) with $U=1.0t$. The lowest curve is for tetragonal symmetry [$\delta=0$ in Eq. (1)]. The energy of the lower edge of this curve is somewhat less than the maximum value of $2\Delta_0$ (Brillouin zone) $=0.4t$ and the upper edge is related to the van Hove energy. This can be clearly seen in the second curve which is for the case $\delta=0.05$ (orthorhombic lattice). In this case, the van Hove singularity splits into two smaller structures which move further apart in the higher curves which apply, respectively, for $\delta=0.10, 0.15, 0.20$, and 0.25 . Each set of curves is displaced upwards by half a unit; relative zeros are shown on the right-hand side. Parameters: first Brillouin zone has $(1000)^2$ points, $T_c=0.1t$, $\Gamma=0.01t$, $\langle n \rangle=0.40$, and $B=0.45$.

height from that at T_c , as the temperature is reduced for the tetragonal and orthorhombic lattices, respectively, and energy gap marked as follows: pure d wave (solid line; $\omega=0.347t$), $0.2s_{x^2+y^2}+0.8d_{x^2-y^2}$ [dotted line; $\omega=0.387t$ (tetragonal), $\omega=0.357t$ (orthorhombic)], and $0.5s_{x^2+y^2}+0.5d_{x^2-y^2}$ [dashed line; $\omega=0.348t$ (tetragonal), $\omega=0.382t$ (orthorhombic)]. In the orthorhombic case, the peak height increases tenfold, while for the tetragonal case, the peak height increases only fivefold.

We can now suggest a decision tree for separating the effects of anisotropy due to the band structure and the energy gap. First, measure the q_x and q_y FWHM at T_c —if they are different, then band structure anisotropy is important. Next, look at the low temperature behavior of the q_x and q_y FWHM of the (π,π) peak. If the system is tetragonal (i.e., direct anisotropy due to band structure effects is not important) with a d -wave energy gap, no difference in the q_x , q_y profiles will be seen. If the system is tetragonal with an anisotropic gap, the FWHM in the perpendicular directions will be different, and that difference will be an estimate of the anisotropy of the gap; the q_y profile will be widest. If the system is orthorhombic (i.e., direct anisotropy due to band structure effects is important) with a d -wave gap, then at low temperatures the difference in widths already present at T_c will have increased considerably (three times in the model considered here) and the q_x profile is widest. If the system is orthorhombic with an anisotropic gap, the difference in widths will increase, but less dramatically. If there is an equal mixture of extended s -wave and pure d -wave energy gap, the ratio of peaks widths will not change much at all,

and will decrease at moderate temperatures. It is clear from the above that it is not so easy to distinguish the symmetric and anisotropic energy gaps on an orthorhombic system. Still, an analysis based on a model of the kind used in this paper could be used to make an estimate of gap admixture, although such an analysis may be model dependent.

Finally, we address the question of how band structure anisotropy itself affects the frequency dependence of the spin susceptibility at \mathbf{q} equal to (π,π) . As a first attempt, we use the single band model of Eq. (1) with finite value of δ , i.e., the hopping parameter in x and y direction in a single CuO_2 plane are assumed to be different. In such a model, the Fermi surface at filling $\langle n \rangle=0.4$ progressively distorts as δ increases and eventually becomes open in the direction perpendicular to the chains while staying closed in the parallel direction. For a finite value of δ , the van Hove singularity, which has energy $-4Bt$ in the tetragonal case, splits into two singularities with energies $-2(2B \pm \delta)t$. In Fig. 4, we show the frequency dependence (ω) of the imaginary part of the spin susceptibility for a pure d -wave model with $U=1.0t$. The energy on the horizontal axis is in units of t . Each curve has a sharp peak at ω slightly less than the maximum of $2\Delta_0$ on the Fermi surface—this determines the frequencies used in the earlier figures. (See Ref. 14 for a discussion of other aspects of the frequency spectrum.) The curves are for different values of δ starting at $\delta=0$ (bottom curve) and going up to $\delta=0.25$ (top curve), with increments of 0.05 . The lower curve shows an onset at an energy slightly less than twice the maximum gap value on the Fermi surface at zero temperature $2\Delta_0=0.358t$ and a structure (shoulder)

at about $0.69t$ associated with the van Hove singularity.^{8,9} That this structure is due to the van Hove singularity is clear in the upper curves for finite δ (see arrows). As δ increases, the van Hove shoulder splits and the two shoulders move apart. The width of this split is less than 4δ (the difference in energies of the van Hove singularities) even when $U=0$ (not shown). The curves are all calculated at the point $\mathbf{q}=(\pi,\pi)$ in the two-dimensional CuO_2 Brillouin zone and the filling is fixed at $\langle n \rangle=0.4$. This means that the chemical potential shifts slightly ($\sim 1\%$) from curve to curve because the band structure is different.

Within a simple one band model for the electron dispersion relation, we have calculated the effect of both band structure anisotropy and of a mixture of extended s and d wave in the gap function, on the spin dynamics of $\text{YBa}_2\text{Cu}_3\text{O}_7$. We have found that the anisotropy in the dispersion relation has the opposite effect on the momentum space anisotropy of the spin susceptibility peak at $\mathbf{q}=(\pi,\pi)$ than does gap function admixture. Our results are consistent with those of Dai *et al.*,⁷ but we can draw no conclusion from this. Data similar to that taken by Dai *et al.*⁷ on untwinned crystals could be used, in principle, to determine the admixture of $s_{x^2+y^2}$ symmetry with majority $d_{x^2-y^2}$ compo-

nent. A measurable effect is expected on the basis of the c -axis tunneling results of Sun *et al.*²² which imply a 25% admixture of $s_{x^2+y^2}$. This estimate is based on the size of the c -axis Josephson current, which is observed between $\text{YBa}_2\text{Cu}_3\text{O}_7$ and Pb. The observed value of critical current is much reduced over that expected for tunneling between two pure s -wave superconductors. This reduction in critical current fixes the gap admixture. If direct band structure effects are not large, as would be the case if q_x and q_y spin dynamic profiles are not anisotropic in the normal state, the amount of $s_{x^2+y^2}$ admixture can be determined from the amount of splitting observed in the FWHM of the q_x and q_y lines in the superconducting state. If direct band structure effects are large, leading to a significant anisotropy in the normal state, it is more difficult to distinguish this anisotropy from gap admixture anisotropy but it still might be possible to do so although such an analysis would require the use of some model and therefore be model dependent.

This research was supported in part by the Natural Sciences and Research Council of Canada (NSERC) and by the Canadian Institute for Advanced Research (CIAR). We thank C. O'Donovan for important discussion.

-
- ¹J. Rossat-Mignod *et al.*, Physica C **185**, 86 (1991); Physica B **186**, 1 (1993); **192**, 109 (1993).
²J. M. Tranquada *et al.*, Phys. Rev. B **46**, 5561 (1992).
³H. A. Mook *et al.*, Phys. Rev. Lett. **70**, 3490 (1993).
⁴M. Sato *et al.*, J. Phys. Soc. Jpn. **62**, 263 (1993).
⁵B. J. Sternlieb *et al.*, Phys. Rev. B **47**, 5320 (1993).
⁶H. F. Fong *et al.*, Phys. Rev. Lett. **75**, 316 (1995).
⁷P. Dai, H. A. Mook, G. Aeppli, F. Dogan, K. Salama, and D. Lee (unpublished).
⁸Y. Zha and K. Levin (unpublished).
⁹D. Z. Liu, K. Levin, and Y. Zha, Phys. Rev. Lett. **75**, 4130 (1995).
¹⁰K. Levin, Q. Si, Y. Zha, J. H. Kim, and J. P. Lu, J. Phys. Chem. Solids **52**, 1337 (1991).
¹¹Q. Si, Y. Zha, K. Levin, and J. P. Lu, Phys. Rev. B **47**, 9055 (1993).
¹²Y. Zha, K. Levin, and Q. Si, Phys. Rev. B **47**, 9124 (1993).
¹³K. Levin, Y. Zha, R. J. Radtke, Q. Si, M. R. Norman, and H. B.

- Schüttler, J. Supercond. **7**, 563 (1994).
¹⁴M. Lavagna and G. Stemman, Phys. Rev. B **49**, 4235 (1994); G. Stemmann, C. Pepin, and M. Levagna, *ibid.* **50**, 4075 (1994).
¹⁵N. Bulut and D. J. Scalapino, Phys. Rev. Lett. **67**, 2898 (1991); Phys. Rev. B **41**, 1797 (1990).
¹⁶N. Bulut and D. J. Scalapino, Phys. Rev. B **47**, 3419 (1993); **50**, 16 078 (1994).
¹⁷D. Thelen, D. Pines, and J. P. Lu, Phys. Rev. B **47**, 9151 (1993).
¹⁸C. O'Donovan, D. Branch, J. P. Carbotte, and J. Preston, Phys. Rev. B **51**, 6588 (1995).
¹⁹D. Branch and J. P. Carbotte, Phys. Rev. B **52**, 603 (1995).
²⁰C. O'Donovan and J. P. Carbotte, Phys. Rev. B **52**, 4568 (1995).
²¹A. J. Millis, H. Monien, and D. Pines, Phys. Rev. B **42**, 167 (1990).
²²A. G. Sun, D. A. Gajewski, M. B. Maple, and R. C. Dynes, Phys. Rev. Lett. **72**, 2267 (1994).